MEASUREMENT AND CHARACTERIZATION OF CABLE LOSSES FOR HIGH VOLTAGE COAXIAL CABLES USED IN KICKER SYSTEMS

A. Ferrero, CIEMAT, Madrid, Spain

L. Ducimetière, T. Kramer, L. Sermeus, CERN, Geneva, Switzerland

Abstract

In the framework of CERN's LHC Injector Upgrade, simulation models for kicker pulse generators have been improved. A key element in the conventional pulse generators, among many others, are the high voltage coaxial cables. Since they can have significant impact on the waveform characteristics, an accurate cable model for simulation is crucial for reliable results during development. For this purpose, precise measurements of scatter parameters have been carried out in order to improve existing simulation models. Specialized high voltage cables, sometimes SF_6 gas filled, used in various CERN kicker systems are usually large, heavy, not very flexible and often only one end is easy accessible. In addition, the impedance of these cables is rarely of $50\,\Omega$, which presents an extra difficulty. This paper describes the methods that have been defined and used to measure any kind of coaxial structures relying on S11 parameters exclusively. Measurements for various specialized cable types are presented and compared with their improved models. The implications for overall kicker system performance are briefly discussed.

INTRODUCTION

There is a wide variety of kicker systems at CERN and all of them have distinctive features and different performance requirements. Due to this, the coaxial cables used in these systems have very diverse characteristics. Cable impedances from $15\,\Omega$ to $50\,\Omega$ are used and different dielectrics are used according to the operational voltage of each system. All these factors, in combination with the cable geometry, lead to a diverse cable types and therefore a different cable losses response.

The process of setting up a coaxial cable model has been classically based on the information provided by cable manufacturer in the datasheet. Many of these cables were developed and manufactured several decades ago and in the best cases, the provided information contains loss measurements up to only $20\,MHz$. Although this information is useful, it is not sufficient to develop a model suitable to meet the present kicker performance requirements. Hence there is a need to develop a method to measure losses to higher frequencies.

Low Loss Transmission Line

Transmission line losses have been widely studied and plenty of literature can be found covering this topic in detail [1]. The attenuation of a travelling wave inside a coaxial cable of characteristic impedance Z_0, has two different sources and, can be described as shown in Eq. 1.

$$\alpha = \frac{1}{2}\left(\frac{R}{Z_0} + GZ_0\right)\quad \left[\frac{Np}{m}\right] \tag{1}$$

By developing the series resistance R, and the dielectric conductance G, Eq. 2 is obtained.

$$\alpha = \frac{1}{2}\left[\left(\frac{\sqrt{\epsilon_r'}\mu_0 f \pi}{\ln(b/a)\,\eta\sqrt{\sigma}}\right)\left(\frac{1}{a}+\frac{1}{b}\right) + \omega\left(\frac{\sqrt{\epsilon_r'}}{c}\right)\tan(\delta)\right] \tag{2}$$

Where $\eta = \sqrt{\mu_0/\epsilon_0}$ and $\tan(\delta) = (\epsilon_r''/\epsilon_r')$. In addition, a is the outer radius of the inner conductor and b is the inner radius of the outer conductor.

The left hand term, on the right of the Eq. 2 refers to the losses created by the conductors where $\alpha \propto \sqrt{f}$. This term is dependent on both the cable geometry (a, b) and on the conductance σ. The right hand term refers to the dielectric losses. In this case $\alpha \propto f$ and there is no dependence on the cable geometry. Contingent on how both terms depend on f, the conductor and dielectric losses become dominant in different frequency ranges. At low frequencies, conductor losses play a dominant role while, for higher frequencies, the dielectric properties will mostly define the cable attenuation.

MEASUREMENT METHOD

The measured cables are currently in use in CERN equipments. Generally, one of the cable ends is at the surface, connected to the pulse generator, and the other one down in the accelerator tunnel, connected to the magnet. In other cases, the cable is rolled on a drum in a way that only one end is easily accessible for measurements. This is a mayor constraint since no kind of transmission measurement based on S_{12} parameter can be performed. This fact leads to S_{11} measurement as the only possibility to obtain information about the losses. For such measurements an impedance mismatch, at the far end of the cable, allows the attenuated and dispersed waveform to be reflected back towards to the measurement device. The decision to "open circuit" the cable was made, since it is a reliable, easy and repeatable condition at the cable end. However, this introduces a strong measurement limitation specially for large diameter cables. The wavelengths of frequencies above $200\,MHz$ are sufficiently small to let some energy be radiated at the open circuit. Under this circumstances, an ideal open circuit cannot be assumed and the measurement cannot be performed in a reliable way.

If the impedance of the cable (device under test, DUT) is matched with the network analyser (NA), the loss measurement is related to the S_{11} definition (see Eq. 3).

07 Accelerator Technology

T16 Pulsed Power Technology

$$S_{11} = \frac{V_o^+}{V_o^-} = \frac{\Gamma_L V_o^+ e^{-\gamma z}}{V_o^+ e^{+\gamma z}} = \Gamma_L e^{-2\gamma z} \qquad (3)$$

The propagation constant γ is a complex number where the imaginary part represents the phase of the travelling wave. This imaginary part is not of interest here, and can be ignored by selecting only the real component of the parameter S_{11}. To simplify even more the equation, we can assume that the reflection coefficient at the load is $\Gamma_L \approx 1$, in all our range of measurements. Taking this into account, the relation between S_{11} and α can be defined as shown in Eq. 4, where z is the length of the measured cable.

$$\alpha = \frac{ln\left(\Re(S_{11})\right)}{-2z} \qquad (4)$$

However, if the impedance of the DUT is not $50\,\Omega$, which is the most common case, a discontinuity between the NA and the DUT is generated. Figure 1 shows a simplified layout of the cable measurement set up. In addition, the figure illustrates the multiple reflective events under unmatched circumstances. As a consequence of this, the energy coming from the open circuit is masked [2], leading to oscillations in the S_{11} parameter that hide the loss information. To overcome this difficulty, time domain reflectometry (TDR) was applied to the S_{11} parameters. This domain transformation allows to observe the reflective events along the line and gate out the undesired reflections. By doing so, a faked matched condition between the network analyser and the DUT is set, allowing to observe exclusively the open circuit discontinuity and therefore recovering the losses information.
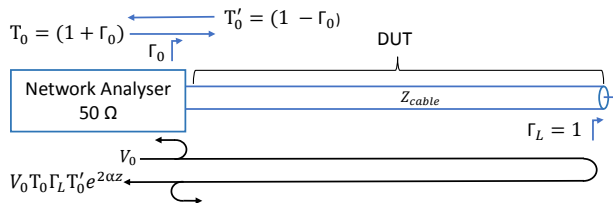
Figure 1: Reflective events layout.

Finally, a scaling factor is applied to Eq. 4 to consider the real amount of energy that has travelled along the cable under unmatched conditions. Regardless of the cable loss, the energy measured by the NA will be attenuated by the transmission factors T_0 and T_0'. Taking this into account we can define then Eq. 5.

$$\alpha = \frac{ln\left(\frac{\Re(S_{11})}{\left(1-\Gamma_0^2\right)}\right)}{-2z} \qquad (5)$$

HV Cable Transition to N Connector

Most of the cables have special high voltage connectors with no standard adapter to a N connector. To properly measure the cables, full custom transitions between both elements were developed. This is a critical element, since the quality of the transition will have a great impact upon

the accuracy of the loss measurement. In addition, it is an element that cannot be easily characterized and, therefore, no error compensation was available. A compact and good design to keep the impedance as constant as possible along the element is fundamental. Figure 2 shows some of the transitions used for this purpose. Note their size differences.
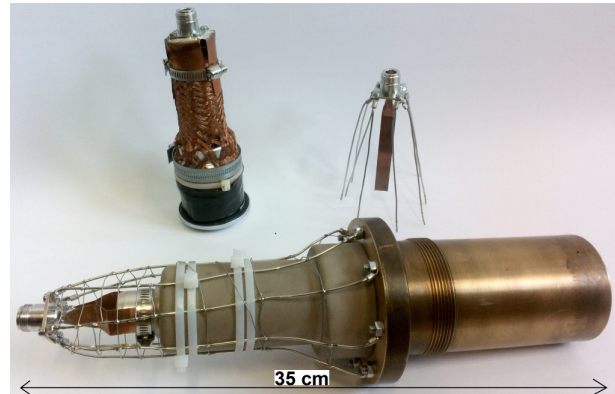
Figure 2: HV coaxial cable to N connector transitions.

MEASUREMENTS RESULTS

To get the maximum accuracy, each measurement was performed with bandwidths of 20 MHz, 50 MHz, 100 MHz and 200 MHz. Subsequently the information was combined to minimize the error and increase the frequency resolution. Figure 3 shows the measured losses for a RG220/U cable of $50\,\Omega$ and for $26.3\,\Omega$ cable from Cable de Lyon (CdL). Both traces agree well with the information provided by the manufacturer.
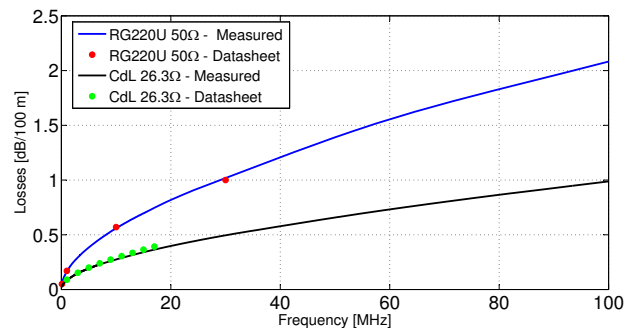
Figure 3: Cable losses comparison between measurements and datasheet information.

In order to compare cable losses, it is necessary to consider several of its physical characteristics. Concerning the conductors, the diameter of the inner conductor plays an important role. Since it is the smallest surface that current will flow through, it decisively contributes to the cable losses. Dielectric insulation also contributes to the losses by parameter G as shown in Eq. 1. Solid dielectrics tend to have a higher $\tan(\delta)$ and ϵ_r' than gas based or foam insulations and have therefore worse performance in the high frequency ranges. Table 1 gathers this information for several cables based on very different technologies. In addition, Fig. 4

plots a comparison of the measured losses for the structures mentioned in Table 1.

Table 1: Measured HV cables Main Parameters

Cable name	Outer / Inner cond. $\varnothing$[mm]	Impedance	Insulation
CdL	50 / 26.5	26.3 Ω	PE + SF_6
CdL	27 / 7.5	52.6 Ω	PE + SF_6
RG220/U	23 / 6.6	50 Ω	PE
F&G	24.6 / 5.6	52.6 Ω	PE + Semicond.
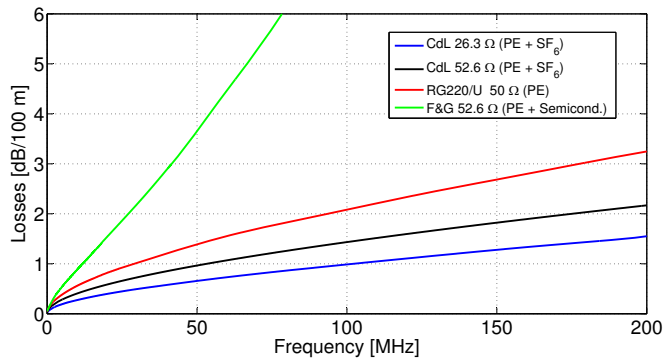
Figure 4: Comparison of coaxial cable measured losses.

According to the results shown by Fig. 4, SF_6 gas filled cables have the best performance. These cables are generally used for very demanding kicker applications and therefore their size and dielectric insulation are chosen to minimize the losses. Concerning CdL 52.6 Ω and RG220/U 50 Ω, these are similar cables from the point of view of geometry and impedance. However, the solid PE insulation of the RG220/U cable degrades its loss performances, especially in the high frequency range. The green trace in Fig. 4 shows the losses behaviour of a semiconductor layer cable. Even if the cable size and impedance are not too far from the RG220/U one, the losses rapidly increase following a 2nd order polynomial function. The high resistance of the semiconductor layers wrapped around the conductors generally increases the losses of this type of cables by a factor of ten.

PSPICE CABLE MODELLING AND SIMULATIONS

To fully describe a cable model, AC and DC cable responses are needed. The DC cable response is either analytically calculated, based on cable geometry and materials specified by the manufacturer, or measured with a four wires sensing procedure. Combined with the AC response measured with the NA, a value for R and G in Eq. 1 was found for each cable. In addition, the $\tan(\delta)$ of the insulation was derived. In the case of semiconducting cables, extra effort was done to define a 2nd order model. Table 2 shows the values used for R, G and $\tan(\delta)$.

Some of the cables studied in this paper are used in the PS injection system (KFA45). A complex PSpice model for this system has been developed at CERN in the past. The new cable models discussed in this paper were included in

Table 2: R and G Parameters for Pspice Cable Models

Cable name	R [Ω/m]	G [Sm^{-1}]	$\tan(\delta)$
CdL 26.3 Ω	$196 \times 10^{-6} + 4.7 \times 10^{-6} * \sqrt{f}$	$188 \times 10^{-15} * f$	160×10^{-6}
CdL 52.6 Ω	$1 \times 10^{-3} + 14.3 \times 10^{-6} * \sqrt{f}$	$108 \times 10^{-15} * f$	184×10^{-6}
RG220/U	$1.5 \times 10^{-3} + 18.6 \times 10^{-6} * \sqrt{f}$	$212 \times 10^{-15} * f$	333×10^{-6}
F&G 26.3 Ω	$1.2 \times 10^{-3} + 8.5 \times 10^{-6} * \sqrt{f} + 19.7 \times 10^{-18} * f^2$	$2.4 \times 10^{-15} * f$	200×10^{-6}

the model and some simulations were run to study the implications for the current pulse. Figure 5 shows a comparison of the effect of the new models on the KFA45 current pulse.
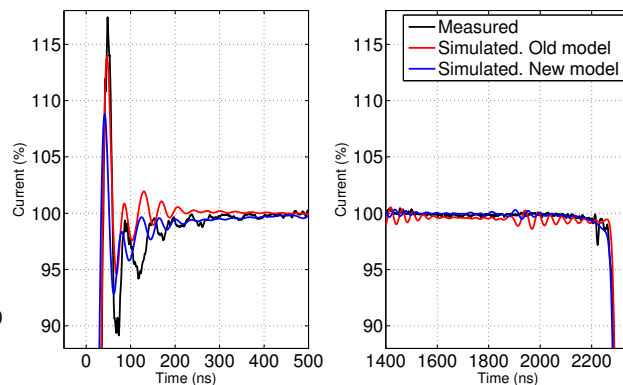
Figure 5: Comparison of the KFA45 current pulse.

Right after the rising edge, the flat top has a slightly positive slope during several hundreds of nanoseconds. This effect has been measured and is related to the attenuation of the higher frequency components of the current pulse. The new cable models describes precisely the response in this range of frequency, leading to a more accurate prediction. Another relevant improvement of the simulation is located in the amplitude of the ripples along the flat top pulse. These ripples are created by several mismatches in the system and are carefully modelled in PSpice in order to reproduce them [3] [4]. Due to the cable losses, these oscillations decay along the pulse length. The new cable models generate an attenuation of the oscillation in much better agreement with the performed measurements in the KFA45.

CONCLUSIONS

A full procedure to precisely measure cable losses has been defined. This method allows to accurately measure the losses of a coaxial cable regardless of its impedance. Historically, an impedance different from 50 Ω was an issue for the deployed procedure. The developed method has been used to measure the losses of coaxial structures in the PS and PSB accelerators. The results were compared with the losses provided by the manufacturer and show an excellent agreement. The measured losses have been used to define better PSpice models and obtain the $\tan(\delta)$ of the dielectric insulation. Finally, PSpice simulations of the KFA45 injection system with the new cable models were carried out. Both models for the old and new cable were compared with measurements confirming a improved accuracy of the simulated current pulse waveform.

REFERENCES

[1] Pozar, D. M. "Lossy Transmission Lines." in *Microwave engineering*. Hoboken, NJ: J. Wiley, 2012, pp. 78-80.

[2] Agilent. "Time Domain Analysis Using a Network Analyser", Application Note 1287-12.

[3] T. Kramer, *et al*., "Feasibility Study of the PS Injection for 2 GeV LIU Beams with an Upgraded KFA-45 Injection Kicker System Operating in Short Circuit Mode", in *Proc. IPAC'16*. Busan, Korea, 2016, paper TUPMR049

[4] Metzmacher, K. D. and Sermeus, L. *et al.*, "The PS Injection Kicker KFA45 Performance for LHC". CERN, Geneva, Switzerland, Rep. CERN-PS-PO-Note-2002-015-Tech, Jan. 2002.